Int. J. Cancer: **122,** 1701–1709 (2008)

FAST TRACK

Mutant p53^{R270H} gain of function phenotype in a mouse model for oncogene-induced mammary carcinogenesis

Christina Heinlein, Frauke Krepulat, Jürgen Löhler, Daniel Speidel, Wolfgang Deppert* and Genrich V. Tolstonog

Department of Tumor Virology, Heinrich-Pette-Institute for Experimental Virology and Immunology, Martinistrasse 52, Hamburg, Germany

In human breast cancer, mutations in the *p53* gene are associated with poor prognosis. However, analysis of patient data so far did not clarify, whether missense point mutations in the *p53* gene, in addition to causing loss of wild-type p53 function, also confer a gain of function phenotype to the encoded mutant p53. As heterogeneity of patient material and data might obscure a clear answer, we studied the effects of a coexpressed mutant p53^{R270H} in transgenic mice in which SV40 early proteins initiate the development of mammary adenocarcinoma (WAP-T mice). In such tumors the endogenous wild-type p53 is functionally compromised by complex formation with SV40 T-antigen, thereby constituting a loss of wild-type p53 function situation that allowed analysis of the postulated gain of function effects of mutant p53^{R270H}. We found that mutant p53^{R270H} in bi-transgenic mice enhanced the transition from intraepithelial neoplasia to invasive carcinoma, resulting in a higher frequency of invasive carcinoma per gland and per mouse, a more severe tumor phenotype, and more frequent pulmonary metastasis. Surprisingly, mutant p53^{R270H} in this system does not increase genomic instability. Therefore, other postulated gain of function activities of mutant p53 must be responsible for the effects described here.

Key words: SV40 early genes; mutant p53 gain of function; mammary carcinoma; tumor progression; transgenic mouse model

About 75% of all mutations in the *p53* tumor suppressor gene comprise missense point mutations.[1] The mutational spectrum of *p53* thus is quite different from that of other tumor suppressors, which are inactivated mostly by gene truncation, deletion or promoter silencing. The findings originally suggested that missense point mutations in the *p53* gene might provide a selective growth advantage for the tumor.[2] The "gain of function" hypothesis for mutant p53 (mutp53) is further supported by various *in vitro* and *in vivo* studies (see Oncogene Reviews).[3] However, while correlative analyses of data from a large cohort of breast tumor patients clearly indicated that *p53* mutations are associated with bad prognosis, studies did not demonstrate an unequivocal difference in the prognosis between loss of function mutations that inactivate the p53 protein, and "hot spot" missense point mutations that are supposed to confer a gain of function phenotype.[4]

Mutp53 gain of function has been addressed in several animal models,[5–8] and has provided unequivocal experimental *in vivo* evidence for such an effect. However, a direct comparison of tumorigenesis induced by targeted oncogene activation in an adult organ under p53 "loss of function" *versus* mutp53 "gain of function" conditions so far had not been performed.

We previously described a transgenic mouse model for mammary adenocarcinoma based on BALB/c mice, because their genetic background favors the development of mammary carcinoma.[9] Transgenic BALB/c mice (WAP-T mice) were constructed that carry the SV40 early gene region under the control of the murine whey acidic protein (WAP)-promoter, which is activated by lactotrophic hormones in differentiating mammary epithelial cells (MEC) during late pregnancy and lactation.[10] As a consequence of transgene expression, WAP-T mice develop multifocal intraepithelial neoplasia, which can further progress to invasive, but rarely metastatic mammary carcinoma. The relevance of this model is emphasized by the close similarity in histology of the mouse tumors with corresponding human tumors.[11] The model represents a p53 "loss of function" setting, as in MEC of induced WAP-T mice the SV40 T-Ag complexes and functionally compromises the endogenous wtp53.[12]

To assess the effects of a coexpressed mutp53 on tumor progression in our WAP-T mice, we constructed transgenic mice in the BALB/c genetic background that carry hemagglutinin (HA)-tagged *mutp53* minigenes with a point mutation equivalent to the human tumor derived hot spot mutation 273H (m270H), also under the control of the WAP-promoter. The construction and phenotypic characterization of the WAP-mutp53 mice has been previously described in detail.[13]

Although mutations in the *p53* gene appear to be rather early events in human mammary carcinogenesis, they are preceded by other genetic lesions.[14,15] Expression of mutp53 thus follows the expression of initiating oncoproteins. To mimic the human situation, we took advantage of our finding that transgenic mutp53 expression in WAP-mutp53 mice not only is controlled by the WAP-promoter, but also by epigenetic mechanisms. Accordingly, we crossed the WAP-mutp53^{R270H} mouse line H22, which due to epigenetic silencing of the transgene does not express mutp53^{R270H} upon induction, with the highly T-Ag expressing WAP-T mouse line T1. Due to T-Ag induced global chromatin remodeling we observed expression of mutp53^{R270H} in about 2–5% of the induced MEC in the bi-transgenic T1-H22 mice.[13] Tumors developing in T1-H22 mice thus will solely arise from MEC expressing T-Ag, as induction of transgene expression initially will only lead to the expression of T-Ag. Mutp53^{R270H} expression then will follow in a certain percentage of initiated MEC.

Material and methods

Animals

All mice were housed and handled in accordance to official regulations for care and use of laboratory animals (UKCCCR Guidelines for the Welfare of Animals in Experimental Neoplasia) and maintained under SPF conditions. Transgenic mice were kept under barrier conditions with a 12 hr light/dark cycle and access to food and water *ad libitum*. BALB/c WAP-T, mono-transgenic line

The first two authors contributed equally to this paper.

Grant sponsors: Deutsche Forschungsgemeinschaft; the Hamburger Stiftung zur Förderung der Krebsbekämpfung; the Fond der Chemischen Industrie; EC FP6 funding; the publication reflects only the authors' views and the Community is not liable for any use that may be made of the information contained therein; Krebsforschung International; Freie und Hansestadt Hamburg and the Bundesministerium für Gesundheit.

Daniel Speidel's current address is: Children's Medical Research Institute, Westmead, New South Wales 2145, Australia.

***Correspondence to:** Department of Tumor Virology, Heinrich-Pette-Institut, Martinistrasse 52, D-20251, Hamburg, Germany.
Fax: +49-040 48051-117. E-mail: wolfgang.deppert@hpi.uni-hamburg.de

Received 7 September 2007; Accepted after revision 29 October 2007
DOI 10.1002/ijc.23317
Published online 18 December 2007 in Wiley InterScience (www.interscience.wiley.com).

(T1)[11] and BALB/c WAP-mutp53^{R270H}, mono-transgenic line (H22)[13] strains were interbred to obtain T1-H22 bi-transgenic animals.

Clinical tumor staging and histological tumor grading

To enable a quantitative comparison of tumor development between the mono- and bitransgenic mouse lines a clinical staging and histological grading system was designed incorporating the recommendations published by the Annapolis consensus conference on mammary pathology of genetically engineered mice.[16]

Macroscopical staging of mammary glands was performed by inspecting the tissue probes with a magnifier lens equipped with a millimeter scale. The mammary glands were designated by numbers on the left body side in rostral–caudal direction (1, cervical; 2, thoracal; 3, abdominal; 4, inguinal) and the right body side in caudal—rostral direction (5, inguinal; 6, abdominal; 7, thoracal; 8, cervical). If multiple tumor nodules were visible, the largest tumor nodule was chosen for staging. The following staging categories were introduced: stage 0, no macroscopic abnormality detected (NAD); Stage 1, diffusely thickened mammary gland; Stage 2, small solid nodules (up to 0.2 cm); Stage 3, tumor 0.3–0.8 cm; Stage 4, tumor $<$1.6 cm; Stage 5, tumor $>$1.6 cm.

Pulmonary metastases were staged likewise by examining spread out whole organs under a magnifier lens on a light box as well as examining stained duplicate cross-sections covering the whole extent of both lungs under a dissecting microscope. The following staging categories for pulmonary metastases were established: Stage M1, micrometastases, ~100 cells/lung section, only detectable under the microscope; Stage M2, diameter $<$ 2 mm; Stage M3, diameter $>$ 3 mm; visible in spread out whole organs on a light box.

For histological grading 5 categories were defined based on the degree of differentiation. Generally accepted grading parameters for mammary carcinoma *e.g.*, mitotic index and nuclear morphology, are not applicable in this experimental system since the transgenic T-Ag *per se* is fundamentally modifying the proliferation activity and chromatin structure. Representative examples depicting tumor morphology by H&E staining, and T-Ag expression by immunohistochemistry (IHC), are shown in Figure 2. In end point analyses (size of the largest tumor $\leq$2.0 cm in diameter, 6–8 months after parturition), the majority of tumors from T1 mice were of grades 1–3, with a rare occurrence of grade 4 tumors. Typically, undifferentiated grade 3 carcinoma show varying degrees of T-Ag expression indicating a beginning T-Ag independent state. This increasing T-Ag independency is reflected in the reduced to absent T-Ag immunoreactivity of grade 4 tumor cells.

Grade 0 (G0): noninvasive, intraepithelial neoplasia (i.e.N.) encompassing different forms of dysplasias, *in situ* carcinoma (such as solid, micropapillary, papillary cribriform or clinging *in situ* carcinoma) and micro invasive or minimal invasive carcinoma originating from i.e.N.

Grade 1 (G1): well differentiated invasive adenocarcinoma subdivided into glandular-acinar, tubular and papillary types.

Grade 2 (G2): moderately to poorly differentiated invasive adenocarcinoma.

Grade 3 (G3): poorly to undifferentiated (solid) invasive adenocarcinoma.

Grade 4 (G4): undifferentiated invasive adenocarcinoma with anaplastic changes.

Representative examples of graded WAP-T associated mammary neoplasia are shown in Figure 2, panels *a–j*. On duplicate stained cross-sections of the mammary glands all distinguishable tumors were enumerated at low magnification and then graded at higher magnifications. Hyperplastic alterations were separately designated as H, and unchanged glandular tissue as NAD (no macroscopic abnormality detected).

Histology and immunohistochemistry

For histological and immunohistochemical investigations established laboratory protocols were used. Tissue specimens were fixed at room temperature overnight with 4% formaldehyde solution containing 1% acetic acid and stored thereafter in conventional 4% formaldehyde solution at 4°C. Fixed tissue specimens were embedded in Paraplast X-TRA (Sherwood Medical) and deparaffinated sections were stained with H&E (Sigma) and periodic acid-Schiff reaction (PAS) (Sigma) according to standard laboratory protocols.

For antigen demasking, deparaffinated sections were treated with heat in a commercial pressure cooker in the presence of an antigen retrieval solution (Citra Plus, Biogenex). Sections then were incubated overnight at 4°C with appropriately diluted primary antibodies. For immunohistochemical tissue localization of SV40 T-Ag polyclonal rabbit anti SV40 large T-antigen (designated R15 anti-SDS-T, as described previously, Ref. 11) was used; whereas HA-tag (influenza virus hemagglutinin) of the mutp53 was detected by polyclonal rabbit anti HA-tag, No. 561.[17] Specifically bound primary antibodies were detected using a highly sensitive alkaline phosphatase- and polymer-conjugated anti-rabbit Ig detection system (Envision, DakoCytomation, and Histofine, Nichirei, respectively). Alkaline phospatase activity was visualized using naphthol AS-BI-phosphate and New Fuchsin (Fuchsin plus substrate-chromogene, DakoCytomation) as substrate. Finally, sections were counterstained with hemalaun and permanently coverslipped. Stained sections were examined under a Zeiss Axiophot2 microscope (Zeiss, Jena, Germany) and digital pictures were taken with a CCD microscope camera "Focus 4000" (INTAS, Göttingen, Germany).

DNA flow cytometry

Thawed nitrogen-frozen tissue samples were mechanically dispersed, washed in PBS (pH 7.4) and fixed in 80% methanol (−20°C). After rehydration in PBS (pH 7.4)/0.1% EDTA, nuclei were stained with 30 mg/ml propidium iodide (PI) in PBS containing 0.3 mg/ml RNase A for 30 min at 37°C. Measurements were made using an EPICS-XL cytometer and System II software (Beckmann Coulter). Fifty thousand events excluding doublets were analyzed per sample. The DNA index (DI) of tumor cells was calculated as the ratio of the major aberrant peak in relation to the diploid peak in the DNA histogram obtained for nuclei of spleen lymphocytes.

Statistical analyses

Fisher exact (one-tail) probability and Yates' χ^2 tests were performed using a web site for statistical computation (http://faculty.vassar.edu/lowry/VassarStats.html).

Results

Mammary carcinogenesis in T1 and T1-H22 mice

The basic features of mammary carcinogenesis in WAP-T mice have been described previously.[11] Mechanistically, SV40 early proteins mainly serve to functionally eliminate p53 and pRb by binding to the large T-antigen (T-Ag), as shown by RNAi experiments.[18] In addition, interaction of small t-antigen with the catalytic subunit of phosphatase PP2A changes the specificity of PP2A by blocking its association with the PP2A regulatory subunit B56,[19] which is required for the regulation of several cancer-associated pathways.[20] Thereby, expression of SV40 early proteins mimics early genetic alterations common in human mammary carcinogenesis. While expression of SV40 early proteins is absolutely required to initiate tumor development, it is not sufficient and requires additional genetic alterations, which arise from the induction of genomic instability by T-Ag.[21,22] Because of dependency on T-Ag expression, mice differing in their degree of T-Ag expression upon induction show differences in tumor incidence and in severity of tumor phenotypes.

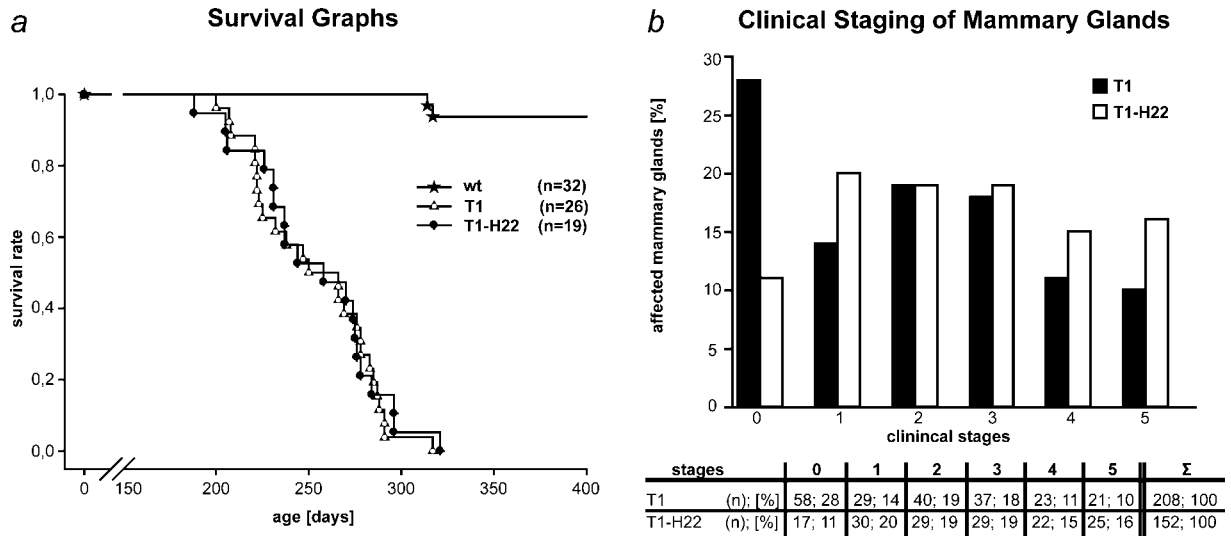

stages		0	1	2	3	4	5	Σ
T1	(n); [%]	58; 28	29; 14	40; 19	37; 18	23; 11	21; 10	208; 100
T1-H22	(n); [%]	17; 11	30; 20	29; 19	29; 19	22; 15	25; 16	152; 100

FIGURE 1 – Survival and clinical staging of mammary glands in transgenic mice. (*a*) Kaplan–Meier curves show no difference in lifetime between the two cohorts of mono-transgenic T1 and bi-transgenic T1-H22 mice (monoparous females). Mice from both transgenic mouse lines have severely reduced life-spans compared to control BALB/c wt animals. (*b*) Clinical staging of macroscopic pathological alterations in 208 murine mammary glands of mono-transgenic T1 (shaded bars) and 152 of bi-transgenic T1-H22 (open bars). Stage 0, no macroscopic abnormality detected (NAD); Stage 1, diffusely thickened mammary gland; Stage 2, small solid nodules (up to 0.2 cm); Stage 3, tumor 0.3–0.8 cm; Stage 4, tumor <1.6 cm; Stage 5, tumor >1.6 cm. The largest tumor amongst multiple tumors per mammary gland was staged.

We here focused on the WAP-T mouse line T1.[11] Long term analysis confirmed that nulliparous WAP-T1 mice develop "spontaneous" mammary carcinoma (1 out of 16; 6%) with the same very low frequency as parental BALB/c mice (3 out of 60; 5%). At 60 days post weaning, T-Ag dependent dysplastic changes and intraepithelial neoplasia, but only very few invasive carcinoma were observed. About 120 days post weaning, most terminal lobular-alveolar units had been converted to intraepithelial neoplasia, and first invasive carcinoma were detected. Multifocal tumor growth was observed from then on, with a latency period of 6 ± 2 months after parturition (Ref. 11 and data not shown). A congeneric pattern of tumor development was observed in bi-transgenic T1-H22 mice (data not shown).

In this respect it is also important to note that, in accordance with previous reports,[13,23,24] mutp53 expression as such does not increase the frequency of mammary tumor development in our WAP-mutp53 mice (5 out of 112; 4%), irrespective of point mutation (R270H or R245W) and expression pattern, compared to parental BALB/c mice (3 out of 60; 5%).

Phenotypic comparison of mammary carcinogenesis in T1 and T1-H22 mice

Latency of tumor formation and survival rates. No difference in latency of tumor formation was observed between induced mono-transgenic T1 and induced bi-transgenic T1-H22 mice. Also the time before the animals had to be sacrificed because of the size of a tumor exceeding 2 cm in diameter, or a bad health or moribund condition, was similar for mono-transgenic and bi-transgenic animals (Fig. 1*a*). As these important features of tumorigenesis were similar in the presence or absence of a coexpressed mutp53^{R270H}, we asked whether the coexpressed mutp53^{R270H} might qualitatively and/or quantitatively affect different stages of mammary carcinogenesis. Therefore, we analyzed in endpoint analyses at about 6–8 months after parturition in detail various phenotypic parameters (see later), using cohorts of 26 T1 and 19 T1-H22 mice.

Clinical staging. Clinical staging of the tumors is a parameter for the severity of the disease at the macroscopic level. Two hundred eight mammary glands from T1 and 152 from T1-H22 animals were screened for pathological alterations and in each affected gland only the largest was staged (see Material and methods section for staging details). Figure 1*b* demonstrates that in T1 mice significantly more glands were macroscopically unaffected (staging 0) than in T1-H22 mice (χ^2 test: $p = 0.0002$), whereas the latter showed a tendency for higher staging (stage 4 and 5) (χ^2 test: $p = 0.0474$).

Histological grading. To assess the pathological severity of the disease, we introduced a histological grading system developed according to the recommendations published by the Annapolis consensus conference on mammary pathology of genetically engineered mice[16] (for details see Material and methods section). Mammary gland cross-sections, in which only intraepithelial neoplasia and *in situ* carcinoma could be detected, were designated as representing grade G0. On the basis of the degree of tumor differentiation, 4 other grading categories encompassing invasive mammary adenocarcinoma were defined (G1–G4). At least 3 mammary glands per mouse from each cohort were analyzed (total of 87 mammary glands from T1, and 79 from T1-H22 mice), and the largest tumor within one mammary gland cross-section was graded. Representative examples depicting tumor morphology by H&E staining, and T-Ag expression by immunohistochemistry (IHC), are shown in Figure 2.

Figure 3*a* shows, firstly, a shift in the histological grading of tumors from differentiated lower (G1 and G2) to undifferentiated higher (G3 and G4) grades in T1-H22 compared to T1 mice, and, secondly, a 2-fold decrease in the fraction of G0 graded glands in bi-transgenic mice. This indicates that mutp53^{R270H} aggravated the severity of the disease by enhanced formation of invasive carcinoma.

Additionally, tumors in individual mammary glands of T1-H22 mice were more heterogeneous regarding their histological grades than tumors in individual mammary glands of T1 mice, as mammary glands of T1-H22 mice contained more tumors with different histological grades than mammary glands in T1 mice (χ^2 test: $p = 0.0341$; Fig. 3*b*).

Mutp53^{R270H} expression increases with tumor grade. Our finding that mammary carcinoma in bi-transgenic mice were of a more severe phenotype prompted us to analyze whether the degree of mutp53^{R270H} expression in mammary carcinoma of T1-H22

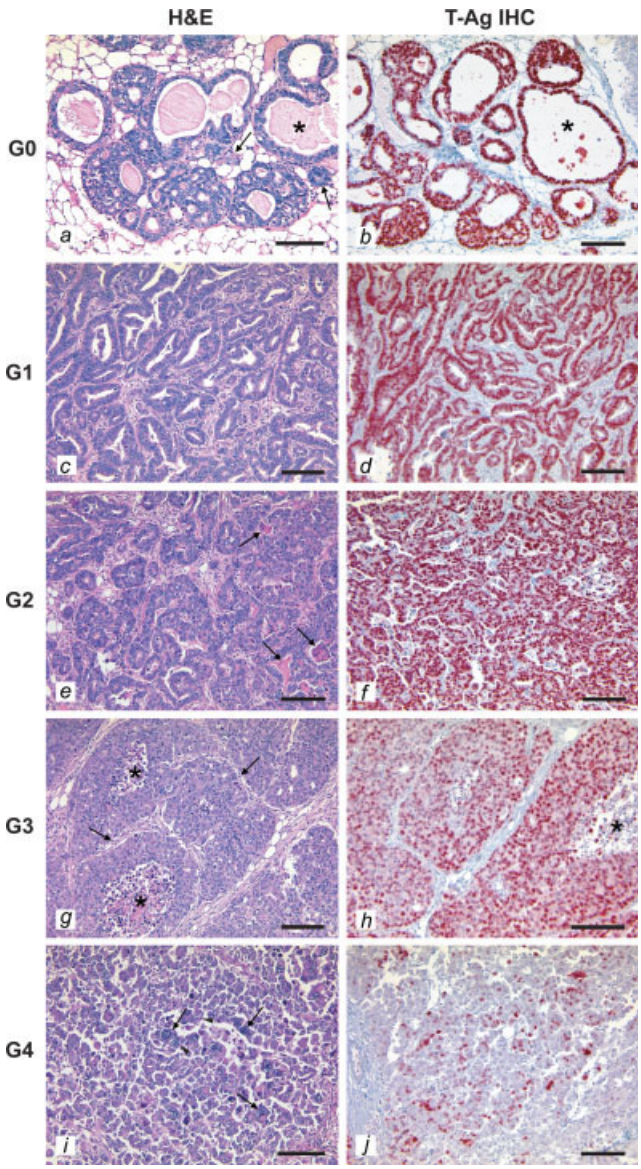

FIGURE 2 – Morphology and T-Ag immunostaining of mammary carcinoma of different histological grades in T1 mice. Sequential sections of pathologically altered mammary glands were stained with H&E (*a*, *c*, *e*, *g*, *i*) and immunostained with polyclonal rabbit antibodies against T-Ag (*b*, *d*, *f*, *h*, *j*). (*a*, *b*), Grade 0: (*a*) End-stage of fully developed intraepithelial neoplasia with typical DCIS-like structures caricaturing the lobular architecture of an expanded TDLU-like murine LA unit (lobulo-alveolar unit). Arrows indicate beginning invasive growth (microinvasive carcinoma). Asterisks mark the greatly dilated lumen of the terminal ductule. (*b*) Nuclear T-Ag staining in the pathologically altered TDLU-like "lobules." (*c*, *d*) Grade 1: (*c*) Well differentiated, invasive tubulo-papillary adenocarcinoma. (*d*) Uniform antibody decoration of tumor cell nuclei. (*e*, *f*) Grade 2: (*e*) Moderately differentiated, invasive tubulo-papillary adenocarcinoma. Arrows indicate comedo necroses. (*f*) Uniform antibody decoration of tumor cell nuclei. (*g*, *h*) Grade 3: (*g*) Relatively monomorphous tumor cells of an invasive adenocarcinoma are arranged in roundish tracts separated by thin septa of stroma (arrows). Centrally located comedo necroses are indicated by asterisks. (*h*) Typically, grade 3 carcinoma show varying degrees of T-Ag expression. (*i*, *j*) Grade 4: (*i*) Invasive mammary carcinoma consisting of discohesively growing, pleomorphous tumor cells with obvious scarcity of stroma. Arrows indicate examples of multinuclear tumor cells, arrow heads nuclear atypias. (*j*) The reduced to absent T-Ag immunoreactivity. Scale bars *a–j* represent: 100 μm.

mice might correlate with tumor grading. Paraffin sections were stained with an HA-tag specific antibody, which specifically detected the mutp53 but not the wtp53 protein. Tumors were classified into 4 expression types based on their staining pattern—none, disseminated, focal, and global. Figure 4*a* shows examples of the respective expression types in intraepithelial neoplasia (panels *a–c*), in differentiated carcinoma (panels *d–f*), and in undifferentiated carcinoma (panels *g–i*). In intraepithelial neoplasia and differentiated carcinoma, the disseminated expression type prevailed. Focal accumulation of mutp53^{R270H} expressing cells was seen at a much lower frequency, and even more rarely global expression of mutp53^{R270H}. In contrast, most undifferentiated tumors showed a focal or global expression of mutp53^{R270H}. Figure 4*b* summarizes the IHC data and shows that the fraction of tumors with focal and global patterns of mutp53^{R270H} staining is significantly (χ^2 test: $p < 0.0001$) higher in undifferentiated G3 and G4 tumors than in intraepithelial neoplasia and in differentiated G1 and G2 tumors. Conversely, the fraction of mutp53^{R270H} negative tumors significantly declines with higher grading.

Frequency of invasive carcinoma. Although no difference in the frequency of intraepithelial neoplasia and in situ carcinoma could be detected between T1 and T1-H22 mice (see earlier), we observed that T1-H22 mice developed more invasive carcinoma than T1 mice, suggesting that mutp53^{R270H} might support the outgrowth of invasive carcinoma. At least three mammary glands from each mouse per cohort were analyzed and all invasive carcinoma per gland (T1: $n = 77$; T1-H22: $n = 75$) were counted. In T1 the maximal number of invasive carcinoma per gland was six, in T1-H22 seven. However, in T1 mice, the majority of mammary glands (89%; $n = 69$) had one or two invasive carcinoma. Only 11% showed more than two invasive carcinoma, whereas in T1-H22 mice 44% ($n = 33$) of mammary glands had more than two invasive carcinoma (from three to up to 7). Given that each T-Ag positive neoplastic lobular-alveolar unit can theoretically transit to invasive carcinoma, we conclude that mutp53^{R270H}, at least in the context of T-Ag driven cell transformation, increases the likelihood of tumor formation by promoting this transition.

Pulmonary metastasis. In a previous study we found that metastasis is rare in T1 mice, and mostly occurs to the lungs.[11] Here we compared the occurrence and staging of pulmonary metastasis in 26 T1 and 19 T1-H22 mice. From each mouse in the cohorts two stained cross-sections covering the whole extent of the lungs were analyzed. Pulmonary metastases were detected in two (8%) T1 and in eight (42%) T1-H22 mice. Whereas the two metastases in T1 mice were of stage M1 (~100 cells/section), one T1-H22 mouse had metastases of stage M2 (diameter < 2 mm), and another one of stage M3 (diameter > 3 mm). Pulmonary metastasis in T1-H22 mice thus is not only more frequent (Fisher's exact test: $p = 0.00848$), but metastases in these mice also grow more aggressively. The increased metastasis in T1-H22 mice is the result of an increased invasiveness, because in contrast to T1 mice, bi-transgenic tumors frequently invade the venous blood system and regional lymph nodes, and infiltrate the surrounding musculature. Representative examples are shown in Figure 5.

Coexpression of mutp53 in T1 mice is not associated with increased genomic instability

During early steps of cell transformation, SV40 T-Ag induces poly- and aneuploidy, thereby initiating chromosomal instability in the developing tumors.[21,22] Recently it has been suggested that mutp53 gain of function is associated with chromosomal instability.[25] Therefore, we expected an additive effect of the coexpressed mutp53^{R270H} on genomic destabilization in the bi-transgenic tumors. To assess the effect, we purified nuclei from uniformly graded tumor tissues (grades 1 to 4) of T1 and T1-H22 mice and stained them with PI and T-Ag-specific antibodies to specifically analyze the ploidy of tumor cells by flow cytometry. The results are shown in Figure 6, where the left hand panels depict the analysis of nuclei from T1 tumors, and the right hand panels that of

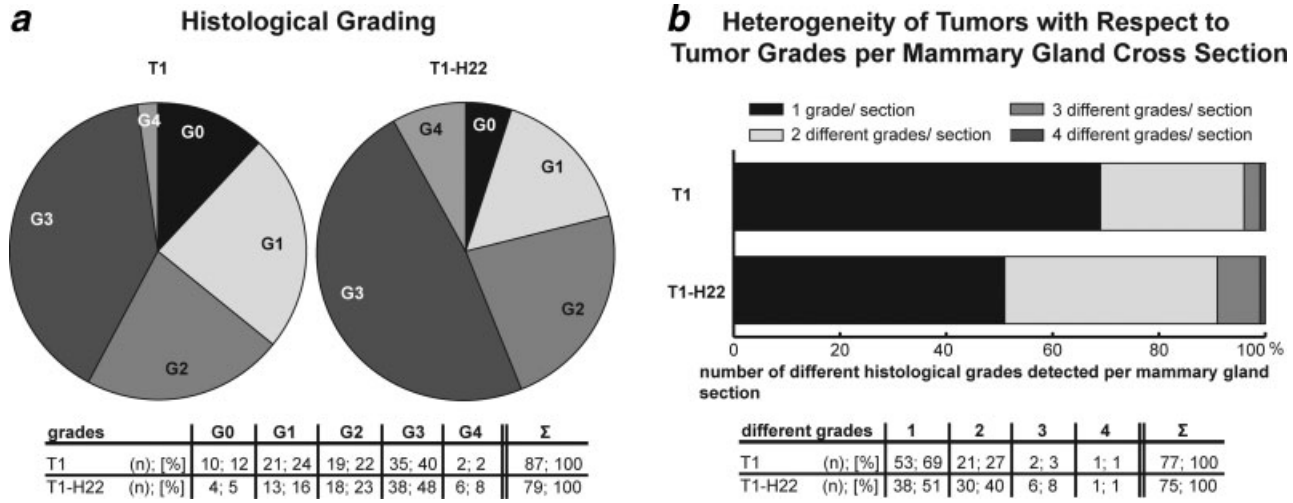

grades		G0	G1	G2	G3	G4	Σ
T1	(n); [%]	10; 12	21; 24	19; 22	35; 40	2; 2	87; 100
T1-H22	(n); [%]	4; 5	13; 16	18; 23	38; 48	6; 8	79; 100

different grades		1	2	3	4	Σ
T1	(n); [%]	53; 69	21; 27	2; 3	1; 1	77; 100
T1-H22	(n); [%]	38; 51	30; 40	6; 8	1; 1	75; 100

FIGURE 3 – Histological grading. (*a*) Histological grades of at least three mammary glands per mouse from each cohort were analyzed (87 from T1 and 79 from T1-H22). All evaluated mammary glands display pathological alterations, implicating intraepithelial neoplasia and minimal invasive mammary carcinoma (G0) as well as invasive mammary carcinoma (G1–G4). The largest invasive mammary carcinoma within one mammary gland cross-section was graded as: G1, well differentiated mammary carcinoma; G2, moderately differentiated mammary carcinoma; G3, poorly to undifferentiated mammary carcinoma; G4, undifferentiated mammary carcinoma with anaplasia. (*b*) Heterogeneity of tumors with respect to histological tumor grades detected within one mammary gland cross-section. Seventy-seven mammary gland sections of T1 and 75 of T1-H22 mice were analyzed and classified according to the number of different histological grades of the tumors observed within one cross-section.

nuclei from T1-H22 tumors. Starting from grade G1, all tumor cell nuclei—except for a small population of T-Ag negative cells with normal DNA content (data not shown)—displayed an aneuploid, but relatively homogenous DNA profile, with a DNA index (DI) ranging from 1.23 to 2.54, indicating a clear prevalence of hyper-diploid cells. Each of the tumors exhibited an individual degree of aneuploidy, reflecting the clonal origin of each tumor. Surprisingly, overall comparison of the DNA profiles did not reveal a significant difference between T1-H22 and T1 tumors. The finding is not compatible with a higher degree of genomic instability in bi-transgenic tumors mediated by mutp53^{R270H}.

Discussion

We here compared mammary carcinogenesis after induction of SV40 early gene expression in the adult mammary gland in the absence or presence of a coexpressed mutp53^{R270H}. In our model, WAP-T mice represent the loss of wild-type p53 function setting in carcinogenesis, while WAP-T x WAP-mutp53 mice represent the corresponding mutp53 gain of function setting in a close to syngeneic background. In mimicking the situation of "spontaneously" arising human mammary tumors, both transgenes are silent during mammary gland development and are expressed exclusively in MEC after induction.

It previously has been suggested that mutp53^{R270H} acts in a dominant-negative manner over endogenous wild-type (wt) p53, rather than exerting a gain of function.[24,26] This certainly applies to situations, where mutp53^{R270H} can form hetero-oligomers with a coexpressed, functionally active wtp53. However, a number of publications[27–30] have demonstrated that in SV40 transformed cells the transactivation activity of wtp53, which is thought to be the major barrier to cellular transformation, is abolished in the presence of SV40 T-Ag, even in the absence of complex formation.[31,32] In addition, complex formation of wild-type p53 with SV40 T-Ag, like the dimerization of p53 monomers, occurs cotranslationally.[33] In contrast, oligomerization of p53, and thereby also hetero-oligomerization of mutp53^{R270H} with wtp53, occurs post-translationally.[33] Furthermore, preliminary evaluation of the effects of a coexpressed mutp53^{R245W} (corresponding to the human ortholog mutp53^{R248W}) in another WAP-T mouse line revealed qualitatively and quantitatively similar results (manuscript in preparation). As mutp53^{R245W} does not hetero-oligomerize with wtp53[34] and our own unpublished observation), we conclude that the effects of mutp53^{R270H} described in this study also reflect a gain of function activity of this protein, although we can not exclude with certainty that so far unknown nontranscriptional activities of noncomplexed, transcriptionally inactive wtp53 in T1-H22 tumors are compromised by mutp53^{R270H}. Most importantly however, even an additional dominant-negative effect of mutp53^{R270H} could not explain the mutp53^{R270H} gain of function phenotype observed here, specifically the 5-fold enhancement of metastasis. Comparative analyses of heterozygous (wtp53+/−) mice with heterozygous mutp53-expressing (mut+/−) mice,[35] and homozygous p53-inactivated (p53−/−) with heterozygous mut+/− mice[36] clearly demonstrated that enhanced metastases is a feature seen only in mutp53 expressing mice, but not in mice in which a *p53* allele had been simply inactivated.

Our comparative analysis showed that mutp53^{R270H} neither decreased latency of tumor formation nor lifetime, but strongly enhanced their progression to invasive mammary carcinoma and aggravated the phenotype of the tumors. Compared to T1 mice, coexpression of mutp53^{R270H} in T1-H22 mice resulted in less macroscopically unaffected glands, a higher incidence of invasive carcinoma per gland and per mouse, and a worse histological tumor grading. Furthermore, an about 5-fold increase in metastasis, and the occurrence of metastases of higher staging was observed in T1-H22 compared to T1 mice.

The findings at first glance seem to correspond well to the previously described transforming activities of mutp53 *in vitro*, where coexpression of mutp53 enhanced the transformation frequency of certain oncogenes.[37] The cooperation of mutp53 with oncogenes so far has been attributed solely to its ability to block the apoptotic, respectively growth repressing functions of wtp53.[38] However, in our system this block is already executed by the SV40 T-Ag, as previously demonstrated.[39] Consistently, mutp53^{R270H} in our transgenic mice did not affect tumor initiation by SV40 T-Ag, as already in T1 mice most lobular-alveolar units in all mammary glands had been transformed to intraepithelial neoplasia and *in situ* carcinoma at about 120 days after induction (parturition). The significant enhancement of transition

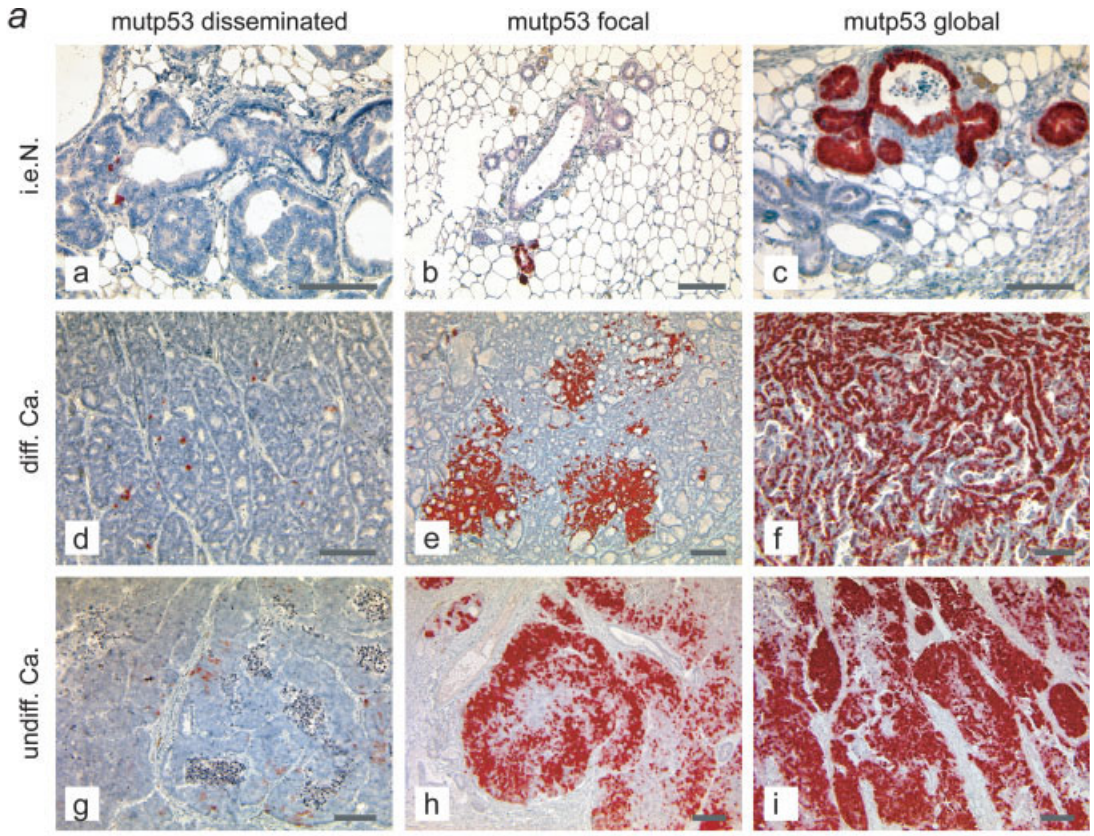

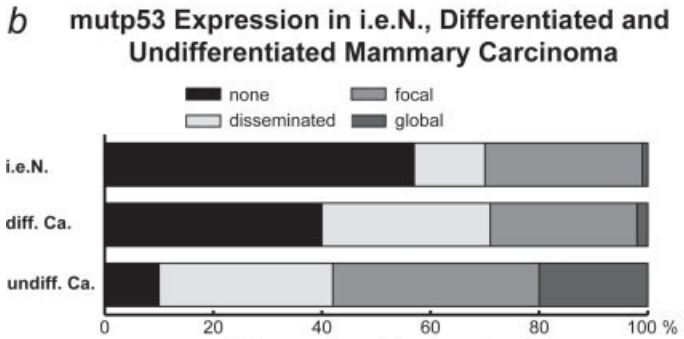

pattern		intraepithelial neoplasia (i.e.N.)	differentiated carcinoma	undifferentiated carcinoma
negativ	(n); [%]	40; 57	21; 40	5; 10
disseminated	(n); [%]	9; 13	16; 31	16; 32
focal	(n); [%]	20; 29	14; 27	19; 38
global	(n); [%]	1; 1	1; 2	10; 20
Σ	(n); [%]	70; 100	52; 100	50; 100

FIGURE 4 – Mutp53 expression pattern in mammary carcinoma of T1-H22 mice. (*a*) Immunohistological expression pattern of mutp53 during tumor progression in bi-transgenic (T1-H22) murine mammary carcinoma. Sections of pathologically altered mammary glands were immunostained with HA-tag specific antibody. (a–i) Disseminated, focal and global mutp53 expression patterns in mammary intraepithelial neoplasia (a–c), differentiated (d–f), and undifferentiated (g–i) mammary adenocarcinoma, respectively. Scale bars represent: 200 μm, (a and c) 100 μm. (*b*) Association of mutp53 expression with higher histological tumor grades. Shown are histograms comparing the percentage of mutp53 immunoreactivity grouped according to expression patterns (negative, disseminated, focal and global) in intraepithelial neoplasia (i.e.N., $n = 70$), differentiated ($n = 52$) and undifferentiated ($n = 50$) mammary carcinoma, respectively.

from T-Ag induced intraepithelial neoplasia to invasive carcinoma by mutp53^{R270H} clearly is a decisive step in tumor progression which constitutes a novel gain of function activity of mutp53^{R270H}. The activity deserves to be further elucidated at the molecular level, as it might be important also in mammary carcinogenesis initiated by other agents.

Any explanation for the effects of mutp53^{R270H} on mammary carcinogenesis in our system so far must remain speculative.

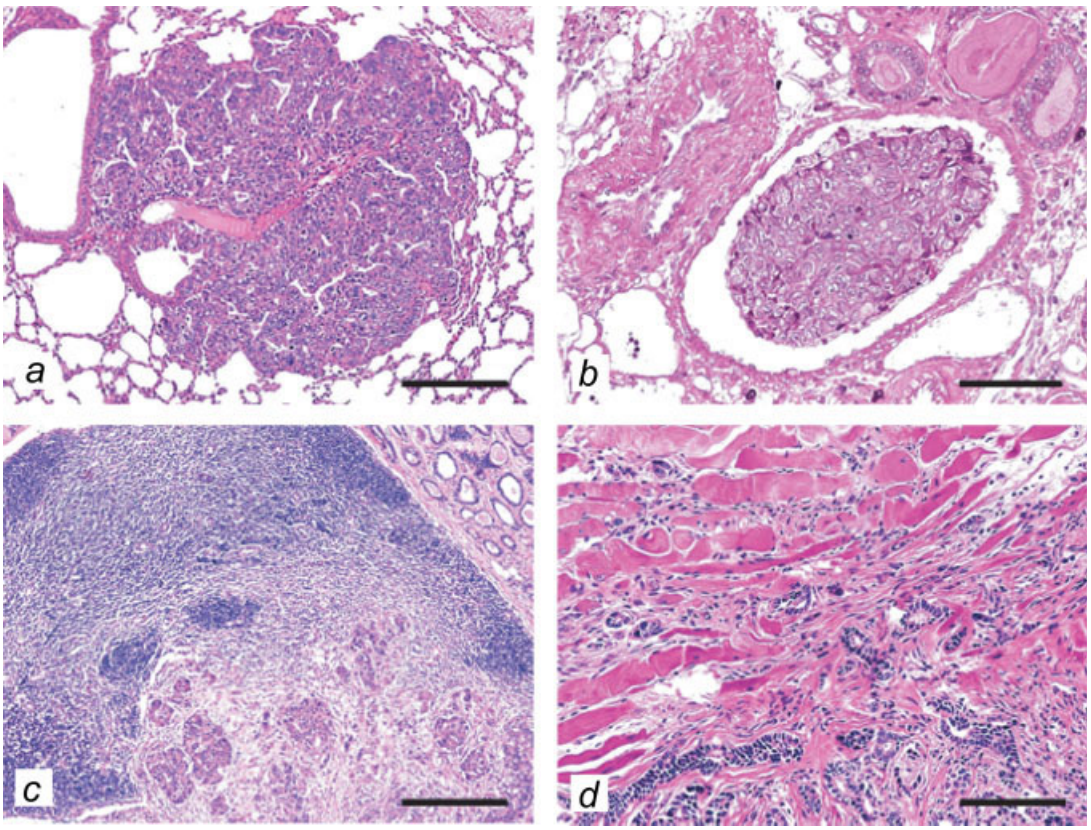

FIGURE 5 – Increased metastasis and enhanced invasiveness of bi-transgenic (T1-H22) murine mammary carcinoma. (*a*) Pulmonary metastasis. (*b*) Tumor tissue in the lumen of a vein. (*c*) Invasion of a regional lymph node. (*d*) Tumor invasion into the musculature. (*a–d*) H&E stain; Scale bars represent: (*a*) 200 μm; (*b–d*) 100 μm.

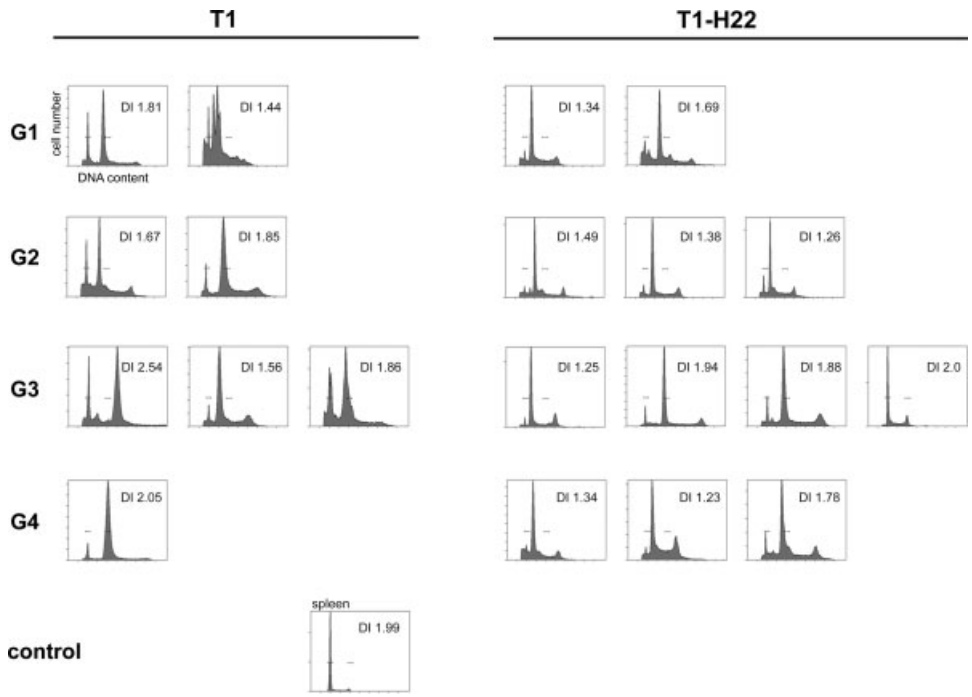

FIGURE 6 – Whole genome analysis of T1 and T1-H22 tumors of different grades by flow cytometry. DNA ploidy of tumor samples (G1–G4) from mono- (T1, left hand panels) and bi-transgenic (T1-H22, right hand panels) animals is shown. DNA fluorescence histograms were obtained by flow cytometry analysis of PI-stained nuclei. Nuclei from spleen cells were used as ploidy standard. DNA index (DI) values for the aneuploid DNA peaks are shown. Horizontal bars in the histograms mark the positions for a G1 and G2 content, respectively.

However, our finding that mutp53^{R270H} in T1-H22 mice furthered the outgrowth of invasive carcinoma from intraepithelial neoplasia and the frequency of metastasis might provide a clue for a possible mechanism. Given that the outgrowth of a tumor from an intraepithelial neoplasia to an invasive carcinoma implies the adaptation of invading tumor cells to a "foreign" environment, one can envision that most cells that cross the basal membrane of an intraepithelial neoplasia will die. Similarly, most disseminated tumor cells will die and not be able to form overt metastases, a phenomenon described as "metastatic inefficiency."[40,41] In these instances, the anti-apoptotic activity demonstrated for human mutp53^{R273H} *in vitro*[42–45] might help the survival of such tumor cells, leading to a higher incidence of invasive carcinoma and of metastases. Interestingly, the so far known anti-apoptotic activities of the mutp53 proteins analyzed do not require genetic alterations, but are mediated by other mechanisms, such as transcriptional regulation of mutp53 target genes,[46] or inactivation of the p53 homologues p63/p73.[47] The rather unexpected finding that T1-H22 tumors showed a similar degree of aneuploidy as T1 tumors thus is compatible with our view. However, the observation seems at variance with a previous report according to which mutp53^{R172H} (the mouse ortholog of the human hot spot mutp53^{R175H}) strongly increases genomic instability in pancreatic tumors.[25] Furthermore, it recently has been shown that human mutp53 can induce genetic instability by disrupting critical DNA damage response pathways, like the ATM pathway.[48] In addition to the fact that quite different systems and different mutp53 proteins were analyzed, it has to be considered that in our system considerable genomic instability is already introduced by the SV40 T-Ag, possibly precluding a further increase in genomic instability.

The finding that mutp53^{R270H} expression in most intraepithelial neoplasia as well as in low grade tumors of bi-transgenic T1-H22 mice is only focal or even disseminated is also compatible with our hypothesis. Detection of mutp53 by IHC requires a certain threshold level of mutp53. Thus mutp53 could be expressed at a low level in all cells and IHC might detect only the few cells expressing mutp53 that was activated at the time of tumor collection.[7] Also in this respect the bi-transgenic tumors in our model reflect the situation in many human tumors with a *mutp53* gene status, but displaying a variegated mutp53 expression in IHC.[49]

The quantitative rather than qualitative effects of mutp53^{R270H} on tumor progression as described in this study could also explain, why a gain of function effect of mutp53 will be difficult to deduce from the analysis of patient data. In our system, a large number of tumors that arose on a genetically homogenous background had to be analyzed to unequivocally demonstrate these effects. Such an analysis is not possible with human tumor material, where in addition to the individual genetic and age differences, different regimens applied for treating the disease have to be considered.

The animal model described here will allow testing our hypothesis on the molecular level, thus shedding further light on the molecular basis of the gain of function described here for mutp53^{R270H}. Such studies are currently underway in our laboratory.

Acknowledgements

The authors thank Ms. Andrea Diesterbeck, Ms. Jasmin Oehlmann and Ms. Silvia Dolski for competent technical assistance, and the staff of the HPI animal quarters for their help. The work described herein is part of the Ph.D. thesis by Dr. C.H., who was supported by a fellowship by Krebsforschung International (KFI), which is gratefully acknowledged. The Heinrich-Pette-Institut is financially supported by the Freie und Hansestadt Hamburg and the Bundesministerium für Gesundheit.

References

1. Soussi T, Kato S, Levy PP, Ishioka C. Reassessment of the TP53 mutation database in human disease by data mining with a library of TP53 missense mutations. Hum Mutat 2005;25:6–17.
2. Hollstein M, Sidransky D, Vogelstein B, Harris CC. p53 mutations in human cancers. Science 1991;253:49–53.
3. Deppert W. Mutant p53 Oncogene, vol. 26. Oncogene. Nature publishing group, The Macmillan Building, 4 Crinan Street, London, NI 9XW, UK, 2007.
4. Olivier M, Langerod A, Carrieri P, Bergh J, Klaar S, Eyfjord J, Theillet C, Rodriguez C, Lidereau R, Bieche I, Varley J, Bignon Y, et al. The clinical value of somatic TP53 gene mutations in 1,794 patients with breast cancer. Clin Cancer Res 2006;12:1157–67.
5. Attardi LD, Donehower LA. Probing p53 biological functions through the use of genetically engineered mouse models. Mutat Res 2005;576: 4–21.
6. Blackburn AC, Jerry DJ. Knockout and transgenic mice of Trp53: what have we learned about p53 in breast cancer? Breast Cancer Res 2002;4:101–11.
7. Iwakuma T, Lozano G. Crippling p53 activities via knock-in mutations in mouse models. Oncogene 2007;26:2177–84.
8. Lozano G. The oncogenic roles of p53 mutants in mouse models. Curr Opin Genet Dev 2007;17:66–70.
9. Kuperwasser C, Hurlbut GD, Kittrell FS, Dickinson ES, Laucirica R, Medina D, Naber SP, Jerry DJ. Development of spontaneous mammary tumors in BALB/c p53 heterozygous mice. A model for Li-Fraumeni syndrome. Am J Pathol 2000;157:2151–9.
10. Andres AC, Schonenberger CA, Groner B, Hennighausen L, LeMeur M, Gerlinger P. Ha-ras oncogene expression directed by a milk protein gene promoter: tissue specificity, hormonal regulation, and tumor induction in transgenic mice. Proc Natl Acad Sci USA 1987;84:1299–303.
11. Schulze-Garg C, Lohler J, Gocht A, Deppert W. A transgenic mouse model for the ductal carcinoma in situ (DCIS) of the mammary gland. Oncogene 2000;19:1028–37.
12. Farmer G, Bargonetti J, Zhu H, Friedman P, Prywes R, Prives C. Wild-type p53 activates transcription in vitro. Nature 1992;358:83–6.
13. Krepulat F, Lohler J, Heinlein C, Hermannstadter A, Tolstonog GV, Deppert W. Epigenetic mechanisms affect mutant p53 transgene expression in WAP-mutp53 transgenic mice. Oncogene 2005;24:4645–59.
14. Bartkova J, Horejsi Z, Koed K, Kramer A, Tort F, Zieger K, Guldberg P, Sehested M, Nesland JM, Lukas C, Orntoft T, Lukas J, et al. DNA damage response as a candidate anti-cancer barrier in early human tumorigenesis. Nature 2005;434:864–70.
15. Borresen-Dale AL. TP53 and breast cancer. Hum Mutat 2003;21: 292–300.
16. Cardiff RD, Anver MR, Gusterson BA, Hennighausen L, Jensen RA, Merino MJ, Rehm S, Russo J, Tavassoli FA, Wakefield LM, Ward JM, Green JE. The mammary pathology of genetically engineered mice: the consensus report and recommendations from the Annapolis meeting. Oncogene 2000;19:968–88.
17. Chuikov S, Kurash JK, Wilson JR, Xiao B, Justin N, Ivanov GS, McKinney K, Tempst P, Prives C, Gamblin SJ, Barlev NA, Reinberg D. Regulation of p53 activity through lysine methylation. Nature 2004;432:353–60.
18. Voorhoeve PM, Agami R. Knockdown stands up. Trends Biotechnol 2003;21:2–4.
19. Moreno CS, Ramachandran S, Ashby DG, Laycock N, Plattner CA, Chen W, Hahn WC, Pallas DC. Signaling and transcriptional changes critical for transformation of human cells by simian virus 40 small tumor antigen or protein phosphatase 2A B56γ knockdown. Cancer Res 2004;64:6978–88.
20. Arroyo JD, Hahn WC. Involvement of PP2A in viral and cellular transformation. Oncogene 2005;24:7746–55.
21. Ramel S, Sanchez CA, Schimke MK, Neshat K, Cross SM, Raskind WH, Reid BJ. Inactivation of p53 and the development of tetraploidy in the elastase-SV40 T antigen transgenic mouse pancreas. Pancreas 1995;11:213–22.
22. Li R, Sonik A, Stindl R, Rasnick D, Duesberg P. Aneuploidy vs. gene mutation hypothesis of cancer: recent study claims mutation but is found to support aneuploidy. Proc Natl Acad Sci USA 2000;97:3236–41.
23. Murphy KL, Rosen JM. Mutant p53 and genomic instability in a transgenic mouse model of breast cancer. Oncogene 2000;19:1045–51.
24. Wijnhoven SW, Zwart E, Speksnijder EN, Beems RB, Olive KP, Tuveson DA, Jonkers J, Schaap MM, van den Berg J, Jacks T, van Steeg H, de Vries A. Mice expressing a mammary gland-specific R270H mutation in the p53 tumor suppressor gene mimic human breast cancer development. Cancer Res 2005;65:8166–73.

25. Hingorani SR, Wang L, Multani AS, Combs C, Deramaudt TB, Hruban RH, Rustgi AK, Chang S, Tuveson DA. Trp53R172H and KrasG12D cooperate to promote chromosomal instability and widely metastatic pancreatic ductal adenocarcinoma in mice. Cancer Cell 2005;7:469–83.
26. Wijnhoven SW, Speksnijder EN, Liu X, Zwart E, vanOostrom CT, Beems RB, Hoogervorst EM, Schaap MM, Attardi LD, Jacks T, van Steeg H, Jonkers J, et al. Dominant-negative but not gain-of-function effects of a p53.R270H mutation in mouse epithelium tissue after DNA damage. Cancer Res 2007;67:4648–56.
27. Bargonetti J, Reynisdottir I, Friedman PN, Prives C. Site-specific binding of wild-type p53 to cellular DNA is inhibited by SV40 T antigen and mutant p53. Genes Dev 1992;6:1886–98.
28. Jiang D, Srinivasan A, Lozano G, Robbins PD. SV40 T antigen abrogates p53-mediated transcriptional activity. Oncogene 1993;8:2805–12.
29. Wahl AF, Donaldson KL, Fairchild C, Lee FY, Foster SA, Demers GW, Galloway DA. Loss of normal p53 function confers sensitization to Taxol by increasing G2/M arrest and apoptosis. Nat Med 1996;2:72–9.
30. Dobbelstein M, Roth J. The large T antigen of simian virus 40 binds and inactivates p53 but not p73. J Gen Virol 1998;79(Part 12):3079–83.
31. Rushton JJ, Jiang D, Srinivasan A, Pipas JM, Robbins PD. Simian virus 40 T antigen can regulate p53-mediated transcription independent of binding p53. J Virol 1997;71:5620–3.
32. Technau A, Wolff A, Sauder C, Birkner N, Brandner G. p53 in SV40-transformed DNA-damaged human cells binds to its cognate sequence but fails to transactivate target genes. Int J Oncol 2001;18:281–6.
33. Nicholls CD, McLure KG, Shields MA, Lee PW. Biogenesis of p53 involves cotranslational dimerization of monomers and posttranslational dimerization of dimers. Implications on the dominant negative effect. J Biol Chem 2002;277:12937–45.
34. Lilyestrom W, Klein MG, Zhang R, Joachimiak A, Chen XS. Crystal structure of SV40 large T-antigen bound to p53: interplay between a viral oncoprotein and a cellular tumor suppressor. Genes Dev 2006;20:2373–82.
35. Olive KP, Tuveson DA, Ruhe ZC, Yin B, Willis NA, Bronson RT, Crowley D, Jacks T. Mutant p53 gain of function in two mouse models of Li-Fraumeni syndrome. Cell 2004;119:847–60.
36. Lang GA, Iwakuma T, Suh YA, Liu G, Rao VA, Parant JM, Valentin-Vega YA, Terzian T, Caldwell LC, Strong LC, El-Naggar AK, Lozano G. Gain of function of a p53 hot spot mutation in a mouse model of Li-Fraumeni syndrome. Cell 2004;119:861–72.
37. Deppert W. The yin and yang of p53 in cellular proliferation. Semin Cancer Biol 1994;5:187–202.
38. Levine AJ. The p53 tumor suppressor gene and gene product. Princess Takamatsu Symp 1989;20:221–30.
39. Ahuja D, Saenz-Robles MT, Pipas JM. SV40 large T antigen targets multiple cellular pathways to elicit cellular transformation. Oncogene 2005;24:7729–45.
40. Weiss L. Metastatic inefficiency. Adv Cancer Res 1990;54:159–211.
41. Fidler IJ, Hart IR. Biological diversity in metastatic neoplasms: origins and implications. Science 1982;217:998–1003.
42. Weisz L, Damalas A, Liontos M, Karakaidos P, Fontemaggi G, Maor-Aloni R, Kalis M, Levrero M, Strano S, Gorgoulis VG, Rotter V, Blandino G, et al. Mutant p53 enhances nuclear factor κB activation by tumor necrosis factor alpha in cancer cells. Cancer Res 2007;67:2396–401.
43. Vikhanskaya F, Lee MK, Mazzoletti M, Broggini M, Sabapathy K. Cancer-derived p53 mutants suppress p53-target gene expression—potential mechanism for gain of function of mutant p53. Nucleic Acids Res 2007;35:2093–104.
44. Bossi G, Lapi E, Strano S, Rinaldo C, Blandino G, Sacchi A. Mutant p53 gain of function: reduction of tumor malignancy of human cancer cell lines through abrogation of mutant p53 expression. Oncogene 2006;25:304–9.
45. Blandino G, Levine AJ, Oren M. Mutant p53 gain of function: differential effects of different p53 mutants on resistance of cultured cells to chemotherapy. Oncogene 1999;18:477–85.
46. Weisz L, Oren M, Rotter V. Transcription regulation by mutant p53. Oncogene 2007;26:2202–11.
47. Li Y, Prives C. Are interactions with p63 and p73 involved in mutant p53 gain of oncogenic function? Oncogene 2007;26:2220–5.
48. Song H, Hollstein M, Xu Y. p53 gain-of-function cancer mutants induce genetic instability by inactivating ATM. Nat Cell Biol 2007;9:573–80.
49. Ebina M, Martinez A, Birrer MJ, Ilona Linnoila R. In situ detection of unexpected patterns of mutant p53 gene expression in non-small cell lung cancers. Oncogene 2001;20:2579–86.